Appl. Phys. B 75, 471–476 (2002)
DOI: 10.1007/s00340-002-1003-8

Applied Physics B
Lasers and Optics

C. PÉPIN
S. MARENGO
D. HOUDE✉

Properties of an ultrashort-pumped near-IR high gain dye amplifier

Département de Médecine Nucléaire et de Radiobiologie, Faculté de Médecine, Université de Sherbrooke, Sherbrooke, Québec, Canada J1H 5N4

Received: 12 December 2001/Revised version: 13 May 2002
Published online: 25 October 2002 •

ABSTRACT An ultra-short-pumped optical dye amplifier operating in the near-IR (720 nm) has been developed. We present an experimental study of the input–output characteristics of this simple device in a traveling wave collinear configuration. In essence, the combined effects of the ultrafast nature of the anisotropy induced by the exciting laser pulse along with the short transit time across the length of the cell allow for optimal output conditions given the number of molecules in the active volume. Two distinct amplifying regimes have been observed depending on photon density. Typical gain values of 10^4 of the narrow bandwidth (~ 9 nm) subpicosecond output signal were measured. The 8-mm^2 beam cross section enables this photon amplifier to be utilized in time-gated imaging applications.

PACS 42.60.Da; 42.60.Lh; 42.55.Mv

1 Introduction

Despite the remarkable progress in solid-state laser technology in recent years, applications of dye lasers and amplifiers in fundamental and applied research still abound. Current studies mainly focus on high average power dye amplifier designs [1, 2], on two-photon pumping amplification [3] and to a large extent on transversely pumped thin films [4, 5] or flowing solutions of π-conjugated polymer dyes [6, 7].

It has been stressed in these studies that spectral narrowing or super-narrowing [8] near the spontaneous emission peak wavelength occurs as the pump fluence rises above the stimulated emission threshold value. Concurrently the decay time of the lowest lasing level drastically reduces while this lower limit is exceeded [7]. Most of the liquid solution layouts use short active path lengths and subpicosecond excitation pulses with few passes in the cavity or in a single pass (mirror-less) configuration. The active medium commonly has a filament-like volume with a diameter well below 1 mm.

Our aim is to take advantage of the considerable gain generated by similar techniques to extend them to substantially larger beam diameters that would allow the device to be useful in transillumination time-gated imaging experiments. Image intensifying is one of the most interesting applications of dye lasers. The concept has been tested in the early 1970s with nanosecond lasers and small active volumes. The pioneering work of Hänsch et al. [9] set the pace for other workers in this field.

In this paper, we report the findings gathered from the study of a near-IR dye amplifier with a collimated beam of 8-mm^2 cross section designed for potential time-gated imaging purposes. The input–output properties, gain and spectral bandwidth under ultra-short pumping conditions will be presented. Features such as gain dependence on the time delay between pumping and photon seeding, the presence of a definite threshold fluence and two distinct amplifying regimes, spectral narrowing of the output, the direct link between pump power and dye concentration for maximum yield and finally the response of the amplifier to the input light intensity will be highlighted.

2 Experimental

The set-up for our amplification experiment is shown schematically in Fig. 1. Basically, the amplifying medium is a solution containing the dye molecule at a specific concentration. A subpicosecond exciting pump pulse ($>$ 1-GW peak power) is reduced in size to a 3.2-mm beam diameter and propagates through the dye cell. The illuminated portion of the medium has the shape of a cylinder. After a controlled amount of time, an injection pulse having the same diameter, the same axis of propagation and polarization plane enters the pumped medium and causes the release of energy through stimulated emission along the same direction as the input pulse. The magnified pulse is directed to a monochromator and a silicon photodiode for characterization. The longitudinal amplification scheme can be designed in two different ways: with pump and input pulses in opposite directions or with both pulses moving in the same direction, as illustrated in parts a and b of Fig. 1 respectively. The b configuration was used only once in order to evaluate the differences in gain value and temporal behavior with the a configuration.

The cationic dye molecule 3,3′-dimethyloxatricarbocyanine iodide (DMOTC iodide from Exciton, also referred to as methyl-DOTCI), sometimes used as a saturable absorber, readily dissolves in methanol, a polar solvent, where the iodide anion and the long conjugated chain between

✉ Fax: +1-819/564-5442, E-mail: Daniel.Houde@Usherbrooke.ca

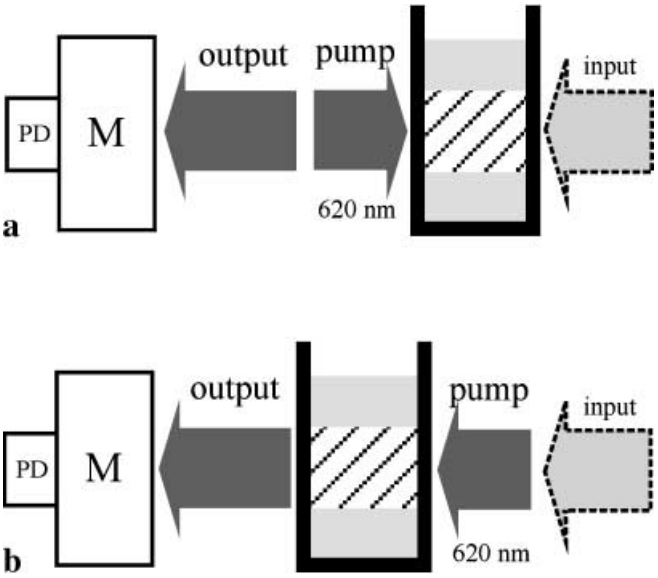

FIGURE 1 Schematic illustration of the experimental set-up. All beams are coaxial and have equal 8-mm^2 circular cross sections. A cylindrical volume inside the 2-mm dye cell is illuminated by a 150-fs pump pulse at 620 nm. Shortly thereafter some input photons penetrate the cell and seed the amplifier. The resulting output light is analyzed by a monochromator (M) and a photo-detector (PD). Two configurations have been tested. In **a** the pump and input pulses travel on a colliding course and in the bottom sketch **b** both travel in the same direction

symmetrical end groups bearing the positive charge easily split. It was chosen because its absorption band is ideally located for our 620-nm pump (extinction coefficient $\varepsilon_{620\,\mathrm{nm}} = 5 \times 10^4\,\mathrm{l\,mole^{-1}\,cm^{-1}}$), which can launch the solute molecules to an excited vibronic level having some excess energy in the S_1 electronic state. A direct reference to the lower excited state lifetime could not be found in the literature, but 1.2 ns has been reported [10] for DODCI in methanol, a close relative of the symmetric carbocyanine family. Excited state absorption studies of HITCI, a dye with the same polymethine chain connected to an indo-type end group, yielded a S_1 lifetime of 1.1–1.2 ns [11, 12]. These values are typical for dyes in the carbocyanine category and it can be assumed that the DMOTC excited state has a comparable fluorescence characteristic time. The peak fluorescence wavelength of 720 nm is well suited for the design of a photon amplifier for near-infrared imaging experiments that are being developed in our laboratory [13]. A fresh solution was prepared from the solid powder before each experiment and circulated through a 2-mm-long fused-silica cell in a constant flow to ensure that an unaltered sample was always present in the illuminated volume.

The 620-nm pump pulse was extracted from a colliding pulse mode-locked (CPM) dye laser followed by four stages of amplification in sulforhodamine and kiton-red dye cells pumped by a 10-Hz frequency-doubled Q-switched Nd:YAG laser from Lumonics. After subsequent compression by a grating pair, typical pulse energies of 0.5 mJ with 150-fs duration can be obtained. A more complete description can be found elsewhere [14]. The femtosecond laser beam originally 10 mm in diameter was reduced in size and collimated to a 8-mm^2 cross section approximately before entering the dye cell. Hence the pump fluence for a 300-μJ pulse is close to 40 μJ/mm^2.

Part of the subpicosecond laser output was redirected and focused into a methanol cell in order to generate a white-light continuum from which pulses with wavelengths of interest were extracted using band pass interference filters (Andover Corp.) and attenuated to the desired intensities with neutral density filters. Because the Kodak Wratten filters that have been used for this purpose absorb less light above 700 nm than their nominal value in the visible region, they were calibrated from 700 to 760 nm so that accurate values of input pulse energies could be determined. Both pump and input pulse intensities have been measured with the Molectron joulemeter model EPM1000 equipped with a J3S-10 silicon probe and all pulse energies were then calculated with the appropriate attenuation factor. The input pulse energy was one of the studied variables in the experiment with values ranging from about 0.5 pJ to 50 nJ. It should be noted that these absolute pulse energies were evaluated using a 30-nm-bandwidth interference filter centered at 720 nm. In fact the measurement represents the integrated fraction of the white-light continuum reaching the detector through this filter. Incident photons of different wavelengths may have different efficiency on the stimulated emission process and some of them may even be inoperative. Consequently, the effective value of the input energy is probably less than specified.

The arrival time of the injection pulse could be controlled by moving an aluminum retroreflector mounted on a precision translation stage and thus the profile of the gain pulse could be recorded as a function of its retardation with respect to the pump. Since the coaxial 620-nm pump and the near-IR amplifier output were traveling along the same path, they were discriminated by a dichroic mirror (CVI Laser Corp.) with a cutoff wavelength of 710 nm. The amplified output pulse was steered to the entrance of a 0.64-m grating spectrophotometer (Instruments SA model HR640) for spectral analysis. Just after the exit slit a silicon photodiode detector (EG & G, DT-100) probed the signal profile according to wavelength or pump-input delay. The steady-state fluorescence spectrum was measured with a Hitachi F-2000 fluorescence spectrometer with $\lambda_{\mathrm{exc}} = 620$ nm.

3 Results and discussion

A measurable amount of time after the passage of the pump through the gain medium, a weak input pulse strikes the excited molecules. The resulting output is the sum of three contributions. First, depending on the dye concentration more or less of the input photons pass through the cell without being absorbed. Second, another part of the output signal can be attributed to ordinary fluorescence or spontaneous decay from the excited singlet level. That contribution can be precisely evaluated by preventing the input from entering the cell and by taking a reading of the detector signal thereafter. Third, the major contribution arises from stimulated emission prompted by the arrival of the injected photons, which seed the excited volume and instigate a coherent avalanche to the fundamental electronic state. The first two components are generally negligible except for low dye concentration or low pump energy conditions. But when both these parameters combine to

provide a high output yield the stimulated emission becomes overwhelming. Amplified spontaneous emission (ASE) also arises at this stage, yielding 5 to 10% of the total output signal. It can however be easily dealt with in the same manner as ordinary fluorescence.

Throughout this paper, the unwanted components of the output signal have been subtracted and only the stimulated emission portion originating from the amplification of the input signal is considered as the effective (or net) output signal. Thus the net amplifier gain is calculated by dividing this reduced value by the input signal intensity. The maximum gain is subject to fluctuations because it is especially sensitive to certain parameters, especially average pump power and interaction cross section, that are not easily reproducible from one experiment to the other. In the high-gain regime, values ranging from 10^3 to 10^5 have been attained with the 2-mm cell in a methanol solution. The pulse width of the magnified pulse has not been measured very precisely. In order to obtain a rough estimation, we used the 720-nm output to bleach a solution of styryl 9M and observed the increase in transmission. The rise time was found to be shorter than 1 ps. Since the bleaching growth represents the convolution of the amplifier output pulse duration with that of the pump, the subpicosecond nature of the amplifier output is thus verified. No further deconvolution of the bleaching slope was performed in order to precisely evaluate the output pulse width.

Let us now consider the magnitude of the (net) output signal as a function of the elapsed time between the pump and the injection pulses under favorable amplifying conditions. Figure 2 illustrates the behavior of the gain curve for the two experimental set-ups as the movable mirror is translated along the axis of propagation. The following description refers to the case where pump and injection are on a colliding course

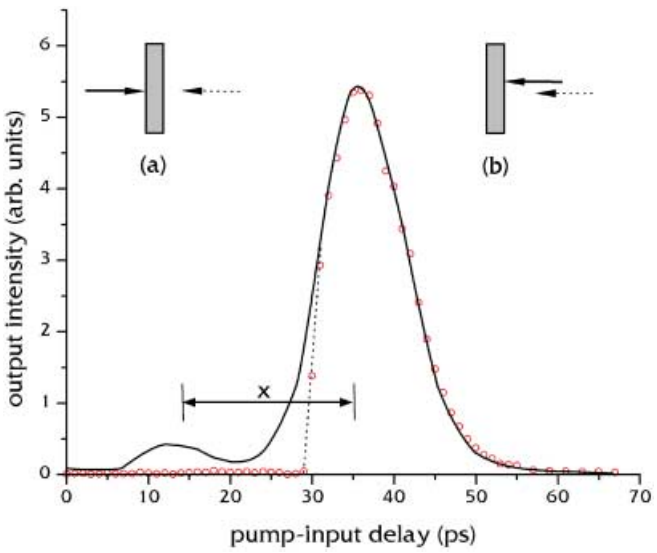

FIGUREE 2 Typical response of the output signal as a function of the delay between the pump and input pulses monitored at 720 nm with the 2-mm cell for both experimental configurations. The gain medium is DMOTC in methanol (concentration: 1.6×10^{-4} M). The zero delay is arbitrary. The *solid curve* describes the signal evolution for the colliding pulse configuration **a** whereas the *open circles* and *dotted line* represent the signal intensity when the input photons follow in the wake of the pump **b**. The maxima of both curves have been given the same intensity to make the shape comparison easier

(Fig. 2a). Each data point represents the time-integrated output intensity as a function of pump-input delay. The origin of the time scale is arbitrary. Maximum intensity (at $\sim$ 35 ps on the graph) results when the pulses meet at a point near the right-hand side of the amplification cell (see Fig. 1). In this nearly optimal situation almost every molecule in the active volume has been promoted to upper energy levels and the incoming faint signal is able to trigger the avalanche. Only those few who have spontaneously migrated down from the lower excited level, mostly from the left-hand side of the cell, do not participate in the process. At the zero-delay position, the input pulse actually goes through the dye solution before the arrival of the pump. Then as the incoming pulse path length is increased the two pulses meet close to the left-hand edge of the cell. At longer delay, while the two meet closer and closer to the right-hand edge, more and more molecules are available for emission, which results in a steady rise of the gain curve. When the gain starts to decrease (at higher delay values) the pump has traversed the whole length of the cell before the arrival of the input pulse. The longer it takes the latter to enter the cell the fewer excited state molecules remain because more of them have departed from the ideal amplifying condition. At some point (small bump on the left), the reflection of the input pulse crosses the pump inside the cell and a significant increase in the signal occurs. The interval x between the small and main peaks is indeed equal to the time taken by light to make a round trip inside the 2-mm methanol cell. This secondary amplification was recorded because of optical feedback due to the cell plane being exactly perpendicular to the laser propagation axis. It can be avoided by slightly tilting the cell.

When comparing the curve profile in both experimental set-ups we find that they are very similar except at the onset. In the 'same-direction' geometry (Fig. 2b), the conclusion that the best situation is when the injection pulse closely follows the pump is manifest. In this codirectional layout, the loss of excited state molecules by spontaneous emission or internal conversion is reduced to a minimum because the input pulse almost immediately stimulates them back to the lower state when the two pulses travel very close together. By virtue of the greater velocity of the injection pulse the steep rise on the left-hand side occurs when they enter the amplifying medium just femtoseconds apart so that the input does not overtake the pump inside the cell. One can expect the rest of the curve to be coincident to that of the 'colliding pulse' geometry because the two situations are similar: the input pulse penetrating the cell after the pump bleaches the whole solution volume. The results examined throughout this paper have been obtained using the configuration where the two pulses propagate in opposite directions. This set-up was adopted because of optical design problems encountered when long scattering paths were needed in order to perform subsequent imaging studies. When operating with the input pulse tracking the pump, very small photon signals would be required to pass through a dichroic mirror while no such impediment exists with the counterpropagation layout.

Two parameters mainly influence the amplifier's operation time: the cell length and the solvent. For longer cells the rise time (left-hand side) lasts longer because the dye concentration is decreased so that the maximum number of molecules

in the cell is of the same order of magnitude as the number of pump photons. Thus to achieve maximum gain for a given pump energy the product of the cell length and the dye concentration is roughly constant. The solvent dependency is illustrated in Fig. 3 where a given DMOTC concentration flows in the same 2-mm cell but in four different increasing chain length alcohols. It can clearly be seen that the decay of the gain curve is directly related to the solvent viscosity in centipoises: 0.544 for methanol, 1.07 for ethanol, 2.03 for isopropyl alcohol and 2.54 for 1-butanol [15]. A similar influence is also noticed in the ascending segment but on a lesser time interval. Such a behavior suggests that the choice of solvent is the determining factor of the amplifier's active period.

Considering the rather lengthy (> 1 ns) fluorescence lifetime of the dye, responsibility for such a short and strong gain duration must be found in another physical cause that involves solvent viscosity. One possible reason could be orientational relaxation. At equilibrium the bulk of dye molecules inside the interaction volume has no special overall alignment. When the polarized pump pulse is present the strong electric field induces an orientation change in this isotropic distribution along its polarization plane. Charged solute molecules are more easily oriented than those with permanent dipoles. While in this state of severe anisotropy, the excited state population can be very efficiently stimulated back to the ground state when triggered by incoming photons polarized along the same plane. As long as this condition prevails high gain can be achieved, but after the passage of the pump the solute molecules will depart from this transient anisotropy and tend to rotate back to their previous random-direction distribution. The time taken to revert to this equilibrium depends on the viscosity of the solvent. After a sufficient amount of time, some small gain can still be possible because in the randomly oriented isotropic solution there are a few molecules in the proper amplifying plane. This small gain regime will last as long as the S_1 population inversion is maintained, i.e. as long as the excited state lifetime.

A prominent aspect of this optical amplifier's performance is the behavior of the gain curve with respect to the pump energy as is depicted in Fig. 4. Below a threshold or quasi-threshold pump intensity of 60–65 μJ, the amplifier losses outweigh the light output by stimulated emission. From 65 μJ to approximately 130 μJ, there is a sudden surge of output energy. In this transition section, there is a thousand-fold increase in yield for twice the invested energy. That constitutes a property similar to conventional cavity lasers, and the amplifier that we are studying could be considered as a mirror-less laser (single-pass laser). As the pump intensity is further increased the gain adopts a more linear dependence until an eventual saturation phase is reached, where a further increment in pump energy becomes ineffectual.

The amplifier can be regarded as having two different modes of operation according to the pulse energy: first a low-gain regime (gain < 100) that can be maintained during a long period of time (> 1 ns) and then a short-lived (10–20 ps) high-gain regime where it behaves in a more linear fashion. It would be more appropriate to consider the pump fluence instead of the pump energy as the important variable in the description of the mode switching, since working with a narrower beam would displace the curves of Fig. 4 to the left if the threshold fluence of $\sim 8\ \mu J/mm^2$ is to be conserved. The threshold feature is indicative of a build-up of energy to a critical 'energy density' that is efficiently discharged when seeded. It may be caused by energy loss from self-absorption or photoisomer absorption. Due to the cation solvation in the polar environment, a minimum amount of energy may be required in order to break up the solvation shell before the solute molecules become free to respond to the strong electric field of the pump pulse.

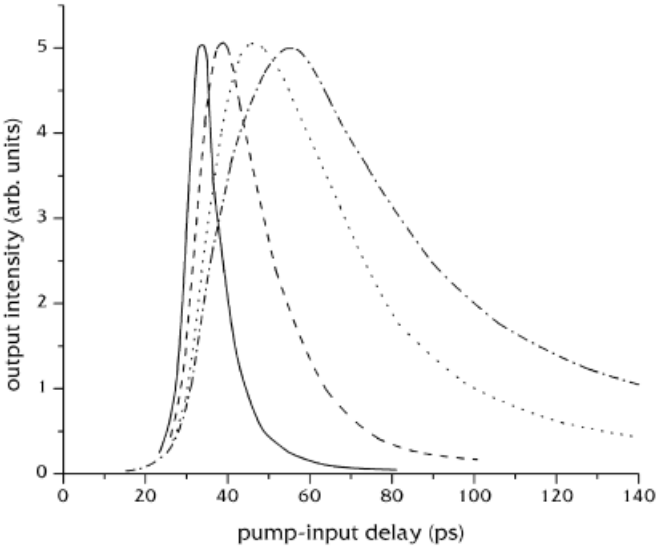

FIGURE 3 Amplifier output signal as a function of the delay between the pump and input pulses monitored at 720 nm with the 2-mm cell for different chain length alcohols used as solvents: methanol (*solid line*), ethanol (*dashed*), isopropyl alcohol (*dotted*) and 1-butanol (*dash-dotted*). The four peak intensities are intentionally assigned the same ordinate value in order to facilitate the comparison between the solvent-dependent rise times and relaxation times

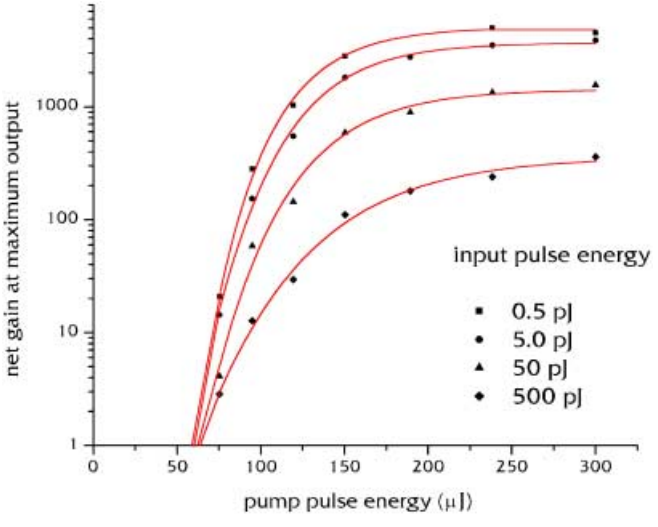

FIGURE 4 Gain curves at peak intensities on a logarithmic scale for the output pulse at 720 nm as a function of the pump pulse energy in a 1.4×10^{-4} M solution of DMOTC in methanol in a 2-mm cell. The collimated beam cross section is 8 mm^2. Each of the four curves shows the gain values for input pulse energies ranging from 0.5×10^{-12} J to 0.5×10^{-9} J. A clear threshold pump energy is found around 60–65 μJ (fluence of approximately 8 $\mu J/mm^2$). After the initial surge the net gain tends to adopt a linear behavior at higher pump fluence

The same experiment has been conducted with four different input pulse energies, the lowest being 0.5 pJ and the largest 500 pJ. Since the net gain is defined as the ratio of the output signal to the input signal, it is logical that the amplifier reaches a higher gain with the lowest input intensity. Nevertheless, ten times fewer input photons do not result in ten times the gain, especially at low photon concentration. Gain saturation limits the efficiency of the amplifier. A greater amount of input photons are necessary to obtain a more productive stimulated emission.

The spectral signature of stimulated emission can be found in Fig. 5. The broad envelope is the steady-state fluorescence spectrum of DMOTC in methanol. Whenever very low concentration or very low pump energy conditions exist the output is a mixture of stimulated and spontaneous emission and the latter is the predominant component, so that the output spectrum resembles this fluorescence contour and the emission is temporally spread out according to the lower excited state lifetime. As the parameters approach threshold values substantial spectral narrowing occurs concurrently with the considerable growth in laser emission. The center wavelength for the high-gain quasi-symmetric band is located very near the steady-state fluorescence peak and has a width of ~ 9 nm at half maximum, which is consistent with the subpicosecond duration of the output pulse. Advantageous high-gain conditions also mean favorable ASE conditions. With the injection pulse blocked, this background ASE was measured as a function of wavelength and its spectrum was found to match the gain spectrum.

On the basis that maximum output is achieved when the number of exciting photons approximately equals the number of dye molecules, one would expect that for a given quantity of pump photons and cell length there exists an optimal concentration where the gain peaks. If the dye is more diluted than this value the population inversion is total and excess pump photons are wasted. If the dye is more concentrated part of the output is quenched by the molecules still lying in the ground state. This fact is illustrated in Fig. 6. Once again the threshold nature of the phenomenon is clearly manifested. Below

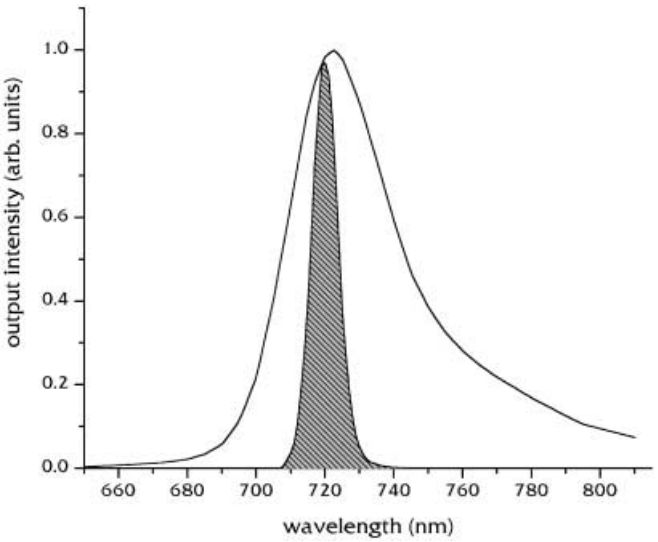

FIGURE 5 Comparison between the spectrum of the steady-state fluorescence of DMOTC and the high-gain amplifier output spectrum (*hashed area*)

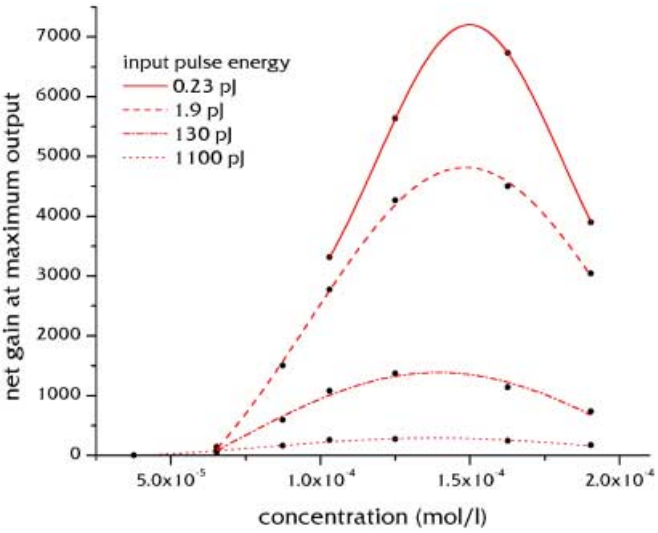

FIGURE 6 Family of curves showing the behavior of the amplifier net gain as a function of the DMOTC methanol solution concentration in a 2-mm-long cell at 720 nm. From *top* to *bottom* the input pulse energy is varied from 0.23 pJ to 1100 pJ. The collimated exciting pulse (620 nm) energy is 300 μJ over an 8-mm^2 area

6.5×10^{-5} M the gain is minimal but at twice that concentration it has almost reached its peak. The ideal concentration (1.5×10^{-4} M in our case) is independent of the amount of input photons provoking the avalanche. As anticipated the output signal quickly drops with an increase in concentration. In our example the molecule count in the active volume is near 10^{15} and a 300-μJ pulse carries approximately 10^{15} 620-nm photons.

Figure 7 displays the same set of variables in a way that is particularly applicable in imaging. Since the input light beam is a few millimeters (~ 3.2 mm) in diameter it can cover a significant area of a heterogeneous object whose various

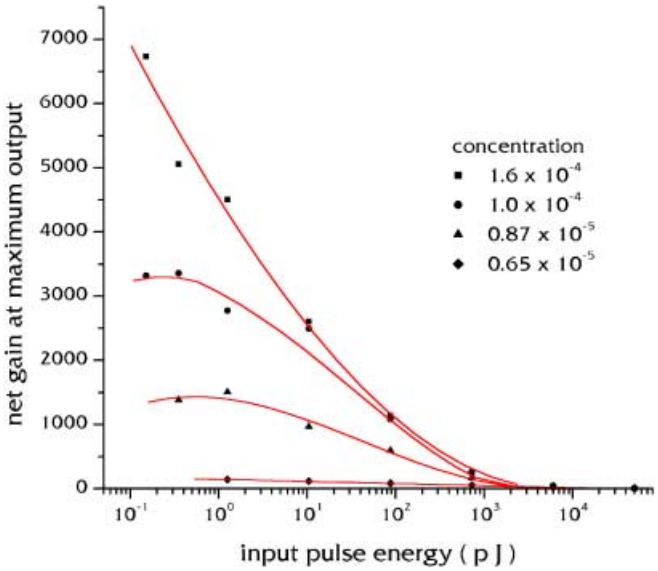

FIGURE 7 Family of curves showing the behavior of the amplifier net gain as a function the energy of the incoming pulse in a 2-mm dye cell containing a solution of different DMOTC/methanol concentrations ranging (from *top* to *bottom*) from 1.6×10^{-4} M to 0.65×10^{-5} M. The collimated exciting pulse (620 nm) energy is 300 μJ over an 8-mm^2 area

parts have different opacities at some specific wavelength. The non-homogeneous light emerging from the illuminated object serves as the amplifier input. Therefore the amplifier response differs depending on the intensity of each pixel in the beam. The object can be reconstructed from the image if the proper gain curve at the working concentration is used in a deconvolution process. This amplifying device having a 10-ps bandwidth has been successfully utilized in time-gated transillumination imaging of objects in scattering media [13]. Only the meaningful group of diffused photons, the first to exit the scattering medium with the proper polarization which carry the useful image information, are strongly magnified while the others are not. This scheme extracts the real image from under the noise in a manner analogous to an electronic lock-in amplifier or phase-sensitive detector.

4 Conclusion

We have developed an 8-mm^2 ultrashort-pumped optical dye amplifier for use in the near IR. It has been shown that there exists a threshold in pump energy and dye concentration for the amplifier to function with at least unit gain. Once this lower limit is exceeded, a low-gain regime occurs characterized by a broad output pulse spectrum and long excited state lifetimes. At still greater pump energy, there appears a regime of solvent-dependent and short-lived high gain with a narrow output spectrum. A background of amplified spontaneous emission also arises in this situation. This strong gain is the consequence of the high transient anisotropy induced by a powerful subpicosecond electric field that tends to align the charged solute. The quantitative description of the amplitude and time evolution of the generated transient gain as a function of all the parameters involved is the subject of further investigation. The solvent viscosity is thought to play a significant role in this regard and special attention will be given to the interplay between fluorescence lifetime, cell length, dye concentration and photon density. Other dyes are also being examined to assess the effect of other molecule-dependent properties.

ACKNOWLEDGEMENTS Funding for this research was provided by the Canadian Institutes of Health Research, by the Canadian Institute for Photonics Innovations and by the Intelligent Materials and Systems Institute.

REFERENCES

1 K. Takehisa: Appl. Opt. **36**, 584 (1997)
2 Y. Maruyama, M. Kato, T. Arisawa: Opt. Eng. **35**, 1084 (1996)
3 R. Weigand, M. Wittman, J.M. Guerra: Appl. Phys. B **73**, 201 (2001)
4 M.D. McGehee, R. Gupta, S. Veenstra, E.K. Miller, M.A. Diaz-Garcia, A.J. Heeger: Phys. Rev. B **58**, 7035 (1998)
5 S.C. Jeoung, Y.H. Kim, D. Kim, J.-Y. Han, M.S. Jang, J.-I. Lee, H.K. Shim, C.M. Kim, C.S. Yoon: Appl. Phys. Lett. **74**, 212 (1999)
6 S.A. van den Berg, G.W. 't Hooft, E.R. Eliel: Phys. Rev. A **63**, 063809 (2001)
7 S.A. van den Berg, R.H. van Schoonderwoerd den Bezemer, H.F.M. Schoo, G.W. 't Hooft, E.R. Eliel: Opt. Lett. **24**, 1847 (1999)
8 S.V. Frolov, Z.V. Vardeny, K. Yoshino, A. Zakhidov, R.H. Baughman: Phys. Rev. B **59**, R5284 (1999)
9 T.W. Hänsch, F. Varsanyi, A.L. Schawlow: Appl. Phys. Lett. **18**, 108 (1971)
10 C.V. Shank, E.P. Ippen: Appl. Phys. Lett. **26**, 62 (1975)
11 A. Müller, J. Schulz-Hennig, H. Tashiro: Appl. Phys. **12**, 333 (1977)
12 G. Beddard, T. Doust, G. Porter: Chem. Phys. **61**, 17 (1981)
13 S. Marengo, C. Pépin, T. Goulet, D. Houde: IEEE J. Sel. Top. Quantum Electron. **5**, 895 (1999)
14 D. Houde, C. Pépin, T. Goulet, J.-P. Jay-Gerin: *Mode-Locked and Solid-State Lasers, Amplifiers and Applications* (Proc. SPIE **2041**) (International Society for Optical Engineering, Washington 1993) p. 139
15 J.P. Jay-Gerin, C. Ferradini: J. Chim. Phys. **91**, 173 (1994)